MENU 2007
11th International Conference
on Meson-Nucleon Physics and
the Structure of the Nucleon
September10-14, 2007
IKP, Forschungzentrum Jülich, Germany

TWO-PION-EXCHANGE EFFECTS IN $pp \to pp\pi^0$ REACTION

F. Myhrer
Dept. of Physics and Astronomy
University of South Carolina
Columbia, SC 29208, USA

Abstract

We study the $pp \to pp\pi^0$ reaction near threshold based on heavy-baryon chiral perturbation theory. We show that the two-pion-exchange diagrams give much larger contribution than the one-pion-exchange diagram which is of lower chiral order in Weinberg's counting scheme. We also discuss the relation of our results to the momentum counting scheme.

The near-threshold $pp \to pp\pi^0$ reaction has been attracting much theoretical attention, ever since experimental data of extremely high quality became available [1]. The heavy-baryon chiral perturbation theory (HBχPT) offers a possible systematic approach to the investigation of this reaction. A motivation of this study may be stated in reference to the generic $NN \to NN\pi$ processes near threshold. Although HBχPT presupposes the small size of its expansion parameter Q/Λ_χ, the pion-production reactions involve somewhat large energy- and three-momentum transfers even at threshold ($\vec{p}^{\,2} \sim m_\pi m_N$). Therefore, the application of HBχPT to the $NN \to NN\pi$ reactions may involve some delicate aspects, but this also means that these processes may serve as a good test case for probing the limit of applicability of HBχPT. Apart from this general issue, a specific aspect of the $pp \to pp\pi^0$ reaction makes its study particularly interesting. For most isospin channels, the $NN \to NN\pi$ amplitude near threshold is dominated by the pion rescattering diagram where the πN scattering vertex is given by the Weinberg-Tomozawa term, which represents the lowest order contribution. However, a quantitatively reliable description of the $NN \to NN\pi$ reactions obviously requires detailed examinations of the corrections to this dominant amplitude. Meanwhile, since the Weinberg-Tomozawa vertex does not contribute to the pion-nucleon rescattering diagram for $pp \to pp\pi^0$, this reaction is particularly sensitive to higher order contributions and hence its study is expected to

provide valuable information to guide us in formulating a quantitative description of all the $NN \to NN\pi$ reactions.

At threshold the strong (and Coulomb) pp initial and final state interactions have to be considered in these reactions. In our DWBA evaluation the nuclear transition operators are derived using HBχPT, whereas the initial and final state nuclear wave functions are calculated in the standard nuclear physics approach (SNPA). A serious problem encountered in performing such a *hybrid* χPT (for short called EFT* below) calculation of pion production is that the calculation involves uncomfortably high momentum components which are present in the nuclear wave functions. The occurrence of these high-momentum components goes against the tenet of χPT, which presupposes the existence of a momentum cutoff scale, $\Lambda_\chi \simeq 1$ GeV/c. The high momenta arise from two sources. The first source is the large momentum components contained in the distorted initial and final wave functions generated by a so-called high-precision phenomenological NN-potential, V_{NN}; see e.g. Ref. [2](b). The second source of the high momentum behavior originates from higher powers of momentum terms which appear in the transition amplitudes generated by higher χPT diagrams [3,4]. Below we will focus our discussion on these transition amplitudes.

In order to eliminate from the NN wave functions the high-momentum components that lie above the original cutoff scale of χPT, a suitably parameterized cutoff factor is introduced (we make certain the observables are independent of this cut-off). This is admittedly an operational remedy, the foundation of which needs to be examined from a formal point of view. It is also informative and of practical value to examine the use of the "low-momentum regime NN potential", V_{low-k} [5–7]. V_{low-k} is derived from V_{NN} by integrating out the high-momentum components contained in V_{NN}. Since V_{low-k} by construction is free from high-momentum components, its use in an EFT* calculations for pion production should alleviate the "high momentum problem" that plagued the past DWBA calculations. From a purist's point of view this may not be a totally satisfactory approach but we believe that this "pragmatic" method still has its merits. We remark that, as is well known, V_{low-k}s generated from any realistic phenomenological potential lead to practically equivalent half-off-shell NN K-matrices and hence the same NN wave function.

We derived the TPE transition amplitude operators [3] using WeinbergÕs chiral counting scheme with expansion parameter $\epsilon \simeq m_\pi/m_N \simeq 0.15$. We isolated the high-momentum components of these amplitudes using an asymptotic expansion, see Refs. [8, 9]. Hanhart and Kaiser [4] used the

momentum counting scheme (MCS) [10, 11] to evaluate TPE diagrams for the reaction $NN \to NN\pi$. The MCS has the expansion parameter $\tilde{\epsilon} \simeq (m_\pi/m_N)^{1/2} \simeq 0.39$. Unlike Weinberg's chiral counting a subtlety in MCS is that loop diagrams of a given order ν in $\tilde{\epsilon}$ not only contains a contribution of order ν (the "leading" part) but, in principle, can also involve contributions of higher order in $\tilde{\epsilon}$ ("sub-leading" parts). Hanhart and Kaiser evaluated the "leading" part of the lowest MCS-order TPE diagrams and showed that the "leading" parts of the two-pion exchange diagrams, when summed up, cancel among themselves, see also Ref. [12]. We [14] identified the "leading" part of our TPE operators [3] and confirmed this cancellation [8, 9]. As will be discussed below, we have found however that the remainder, or the "sub-leading" parts, of the TPE amplitudes can be at least as large as the one-pion rescattering amplitude [8,9]. We consider it important to re-examine the behavior of MCSÕs "sub-leading" parts of these TPE diagrams in order to see whether they can still be as large as indicated by the phenomenological SNPA success of the Lee-Riska heavy-meson exchange mechanism. In a forthcoming publication [13] we will also consider other chiral correction amplitudes including the contributions from counter-terms needed to regulate the UV behavior of the TPE loop diagrams.

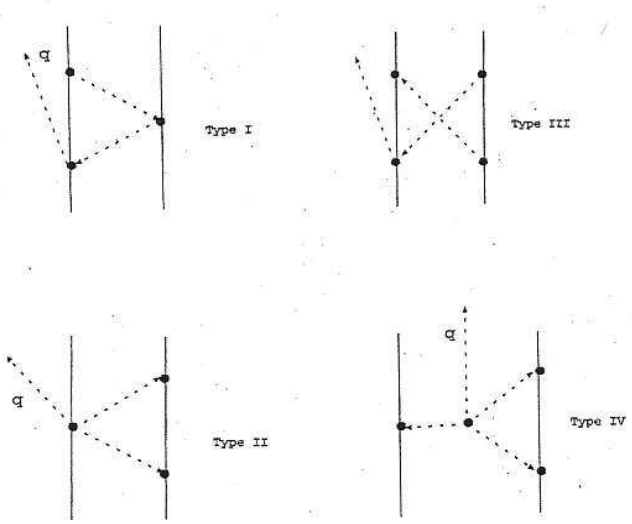

Figure 1: The two-pion-exchange loop-diagrams discussed in the text.

The one-pion loop $pp \to pp\pi^0$ transition operators were evaluated analytically by Ref. [3] using HBχPT. When these operators are sandwiched with phenomenological determined distorted initial and final NN wave functions,

we find that the momentum integrals convergence very slowly [8, 14]. This slow convergence can easily be understood when we adopt the threshold fixed kinematics approximation (*FKA*) to evaluate the amplitudes. We impose the *FKA* on the analytic expressions for the transition operators of the different TPE diagrams are given in Ref. [3] and make an asymptotic expansion in the two-nucleon momentum transfer $\vec{k}$, i.e. $|\vec{k}| = |\vec{p} - \vec{p}\,'| \to \infty$. The transition operator matrix T of the TPE diagrams is of the form

$$T \;=\; \left(\frac{g_A}{f_\pi}\right)\left(\vec{\Sigma}\cdot\vec{k}\right) t(p,p',x) \qquad (1)$$

where $x = \hat{p}\cdot\hat{p}'$. The generic *asymptotic* behavior for $t(p,p',x)$ is [14]:

$$t(p,p',x) \;\overset{k\to\infty}{\sim}\; t_1\big(g_A/(8f_\pi^2)\big)^2\,|\vec{k}| + t_2\,\ln[\Lambda^2/|\vec{k}|^2] + t_3 + \delta t(p,p',x)\;, \qquad (2)$$

where t_3 is asymptotically k-independent, and $\delta t(p,p',x)$ is $\mathcal{O}(k^{-1})$. For each of Types I $\sim$ IV, analytic expressions for t_i's ($i = 1,2,3$) can be extracted [14] from the amplitudes T given in Ref. [3]. The first term with t_1 in eq.(2) is the "leading" term in MCS discussed by HK [4], whereas the remaining terms, which we refer to as the "sub-leading" terms, were not considered by HK.

Table 1: For the four types of TPE diagrams, K= I, II, III and IV, the second row gives the value of t_1 defined in eq.(2), and the third row gives the ratio $R_K = T_K/T_{Resc}$, where T_K is the plane-wave matrix element of T in eq.(1) for Type K, and T_{Resc} is the lowest chiral order one-pion-exchange rescattering (Resc) amplitude. The last row gives $R_K^\star = T_K^\star/T_{Resc}$, where $T_K^\star$ is the plane-wave matrix element of T in eq.(1) with the t_1 term in eq.(2) subtracted.

Type of diagrams : K =	I	II	III	IV	Sum
$(t_1)_K \;\propto$	0	-1	$-1/2$	$3/2$	0
R_K	$-.70$	-6.54	-6.60	9.19	-4.65
$R_K^\star$	$-.70$	-0.82	-3.73	0.60	-4.65

In Table 1, the second row shows that the "leading" parts in the MCS $\propto t_1$ of the TPE diagrams I $\sim$ IV sum to zero. This confirms the finding of Hanhart and Kaiser [4]. In the third row marked R_K, and using *FKA*, we give the values of the ratio of the transition amplitude in Ref. [3] to the rescattering amplitude in the plane wave approximation for the four TPE amplitudes. We note that the sum of the TPE amplitudes are non-zero. The magnitude of the sum reflects the size of the "sub-leading" parts of the TPE amplitudes. In the fourth row we have removed the "leading" term, t_1 from $t(p,p',x)$ in Eq.(1) and then evaluated the similar ratio $R_K^\star$. We observe that

the sum of the four modified TPE amplitudes (II, III and IV) is larger than the rescattering amplitude [8]. This can also be inferred from the R_K row of the table where the ratios of the amplitudes II:III:IV are about -2:-2:3, whereas the ratios of the corresponding amplitudes$\tilde{\text{O}}$ "leading" terms are -2:-1:3. However, the evaluations of the different diagrams appear to confirm that the magnitudes of the different diagrams follow the momentum counting rule as indicated in Table 11 of Ref. [15].

Next we investigate the behavior of the TPE diagrams as we go beyond the plane-wave approximation by using distorted waves (DW) for the initial- and final-state NN wave functions. For formal consistency we should use the NN potential recently derived from HBχPT [16, 17], but as discussed earlier we adopt here EFT*. As argued earlier, in order to stay close to the spirit of HBχPT, we introduce a Gaussian momentum regulator, $\exp(-p^2/\Lambda_G^2)$, in the initial and final distorted wave integrals, suppressing thereby the high momentum components of the phenomenological NN potentials, e.g. the Bonn [18] or Nijmegen potential [19]. We require that Λ_G be larger than the characteristic momentum scale of the $NN \to NN\pi$ reactions, $|\vec{p}| \sim \sqrt{m_\pi m_N} \simeq 360$ MeV/c, but it should not exceed the chiral scale $\Lambda_\chi \sim 1$ GeV/c. Part of the work to implement the idea of utilizing a low-momentum regime NN potential has been published [20] where use was made of V_{low-k}. One issue regarding the use of Stony Brook's V_{low-k} in the present context is that it is derived with a rather low value of the cutoff parameter, $p_{max} = 2$ fm^{-1}, which is very close to the threshold momentum for the $NN \to NN\pi$ reactions. We therefore have extended the V_{low-k} potential to cases where the momentum cut-off p_{max} is allowed to be larger than the original Stony Brook value up to 5 fm^{-1} (this value corresponds to the chiral scale, $\Lambda_\chi \simeq 1$ GeV/c^2). This extended V_{low-k} has been used in our recent study of the two-pion-exchange (TPE) amplitudes for the $pp \to pp\pi^0$ reaction [9].

To evaluate the $pp \to pp\pi^0$ reaction at threshold using HBχPT, the impulse approximation (I.A.) and the one-pion-exchange (Resc) diagrams are the lowest order amplitudes (diagrams) according to Weinberg counting. However, the typical momentum for this reaction at threshold is $p \sim \sqrt{m_\pi m_N}$, which implies that for this reaction we have to take Weinberg chiral counting with a grain of salt. It was shown early on that in HBχPT the I.A. and Resc amplitudes interfere destructively resulting in a very small cross sections [2, 10]. We therefore expect sizeable contributions to this reaction from the TPE diagrams. In Table 2 we show examples, taken from Ref. [9], of DWBA evaluations for a typical energy $T_{lab} = 281$ MeV. Since the t_1 terms add to zero and to improve the numerical convergence, we drop the t_1 terms in our calculations as was done in the fourth row of Table 1.

Thus, in Eq.(1), we use $t^\star(p,p',x)$ instead of $t(p,p',x)$, where $t^\star(p,p',x)$ is obtained from $t(p,p',x)$ by suppressing the t_1 term in Eq.(2). The partial-wave projected form of $t^\star(p,p',x)$ in a DWBA calculation is written as:

$$J = -\left(\frac{m_N m_\pi}{8\pi}\right)\int_0^\infty p^2 \mathrm{d}p\, p'^{\,2}\mathrm{d}p' \int_{-1}^{1} \mathrm{d}x\; \psi_{^1S_0}(p')\; t^\star(p,p',x)\; (p-p'x)\psi_{^3P_0}(p) \quad (3)$$

In Table 2 we show the values of the J amplitudes for each TPE diagram.

Table 2: The values of J, Eq.(3), corresponding to the TPE diagrams of Types I $\sim$ IV, evaluated in a DWBA calculation for $T_{lab} = 281$ MeV. The column labeled "Sum" gives the combined contributions of Types I $\sim$ IV, and the last column gives the value of J for 1π-Resc. For the Nijm93 potential case, the results for three different choices of Λ_G (in MeV/c) are shown. For the case with V_{low-k}, CD-4 (CD-5) represents V_{low-k} generated from the CD-Bonn potential with a momentum cut-off $\Lambda_{low-k} = 4\,\mathrm{fm}^{-1}$ ($5\,\mathrm{fm}^{-1}$). The last row gives the results obtained in plane-wave approximation.

	I	II	III	IV	Sum	1π–Resc
$V_{\rm Nijm}$: $\Lambda_G = 600$	-0.12	-0.12	-0.57	0.07	-0.74	0.20
$V_{\rm Nijm}$: $\Lambda_G = 700$	-0.12	-0.11	-0.57	0.06	-0.74	0.21
$V_{\rm Nijm}$: $\Lambda_G = 800$	-0.12	-0.11	-0.55	0.04	-0.74	0.22
V_{low-k} $(CD-4)$	-0.12	-0.09	-0.46	0.03	-0.65	0.23
V_{low-k} $(CD-5)$	-0.09	-0.06	-0.30	-0.01	-0.46	0.22
Plane$-$waves	-0.06	-0.07	-0.30	0.05	-0.37	0.080

Table 2 shows that the DW amplitudes from the TPE diagrams are only roughly of the order of the one-pion rescattering amplitude tabulated in the last column. Evidently, when we compare to the plane wave amplitudes, the DWBA treatment does affect the relative magnitudes of the various diagrams differently. In the last row we show the plane wave amplitudes and we note that the "sub-leading" part of diagram III is a factor three or more larger than the other amplitudes. The MCS indicates that the "sub-leading" parts of the TPE amplitudes should be of the same order as the one-pion rescattering amplitude. Furthermore, the expansion parameter in MCS, $\tilde{\epsilon} \simeq 0.4$, ideally speaking should be the ratio of the amplitudes from the different orders in the MCS. When comparing the results in Table 1 and Table 2, we find that the "leading" part of diagrams II and IV are almost an order of magnitude larger than their "sub-leading" parts. Clearly, as seen in Table 2, we find, as expected in the MCS, that the amplitudes from the "sub-leading" parts of diagrams II, IV and from the one-pion rescattering diagram are about the

same magnitude. However, diagram III (the "cross-box" diagram) appears not follow the expected MCS behavior. The plane wave amplitude for the "sub-leading" part of diagram III is less than 50% than the "leading" part of diagram III. Moreover, the amplitude of the "sub-leading" part of diagram III is more than a factor $\tilde{\epsilon}^{-1}$ larger than what is expected in the MCS. One explanation could be that we evaluate diagram III using HBχPT's heavy nucleon propagators and not the nucleon propagator which is advocated for the MCS [15]. This issue will be resolved in the near future. A final note, the lowest- and next-chiral-order (diagram VII in Ref. [3]) one-pion-exchange diagrams were found to be same order of magnitude as expected in MCS.

We have demonstrated [9] that, as expected, the two-pion-exchange loop diagrams give very large contributions to the $pp \to pp\pi^0$ reaction at threshold, and that these diagrams will give important contributions to other $NN \to NN\pi$ reaction channels.

Acknowledgments

This research has been done in a close collaboration with Drs. Y. Kim, K. Kubodera and T. Sato. This work is supported in part by the National Science Foundation, Grant No. PHY-0457014.

References

[1] H. O. Meyer *et al.*, Phys. Rev. Lett. **65**, 2846 (1990).

[2] B.-Y. Park, F. Myhrer, J.R. Morones, T. Meissner and K. Kubodera, Phys. Rev. C, **53**, 1519 (1996); T. Sato, T.-S.H. Lee, F. Myhrer and K. Kubodera, Phys. Rev. C, **56**, 1246 (1997).

[3] V. Dmitrašinović K. Kubodera, F. Myhrer and T. Sato, Phys. Lett. **B 465**, 43 (1999).

[4] C. Hanhart and N. Kaiser, Phys. Rev. C, **66**, 054005 (2002); [nucl-th/0208050].

[5] E. Epelbaoum, W. Glöckle and U.-G. Meissner, Phys. Lett. B, **439**, 1 (1998); E. Epelbaoum, W. Glöckle, A. Krüger and U.-G. Meissner, Nucl. Phys. A, **645**, 413 (1999).

[6] M.C. Birse, J.A. McGovern and K.G. Richardson, Phys. Lett. B, **464**, 413 (1999); T. Barford and M.C. Birse, AIP Conf. Proc. **603**, 229 (2001)

[7] S. Bogner, T.T.S. Kuo and L. Coraggio, Nucl.Phys. A, **684**, 432c (2001); S.K. Bogner *et al.*, Phys. Lett. B, **576**, 265 (2003) [nucl-th/0108041]; S. Bogner *et al.* Phys. Rept. **386**, 1 (2003); J.D. Holt *et al.*, Nuc. Phys. A, **733**, 153 (2004).

[8] F. Myhrer, "Large two-pion-exchange contributions to the $pp \to pp\pi^0$ reaction", *to appear in* Proc. Intern. Workshop *Chiral Dynamics 2006*, Eds. M.W. Ahmed *et al.*, World Scientific) [nucl-th/0611051].

[9] Y. Kim, T. Sato, F. Myhrer and K. Kubodera, Phys. Lett. B, to appear; arXiv:0704.1342 [nucl-th] (2007).

[10] T.D. Cohen, J.L. Friar, G.A. Miller and U. van Kolck, Phys. Rev. C, **53**, 2662 (1996).

[11] C. Hanhart, G.A. Miller and U. van Kolck, Phys. Rev. Lett. **85**, 2905 (2000).

[12] V. Lensky, J. Haidenbauer, C. Hanhart, V. Baru, A. Kudryavtsev and U.-G. Meissner, Eur. Phys. J. **A27**, 37 (2006) [nucl-th/0511054]; V. Lensky *et al.*, [nucl-th/0609007]

[13] Y. Kim, T. Sato, F. Myhrer and K. Kubodera, "Two-pion-exchange and the $pp \to pp\pi^0$ cross section", manuscript in preparation.

[14] T. Sato and F. Myhrer, private communication (1999).

[15] C. Hanhart, Phys. Rep. **397**, 155 (2004)

[16] P.F. Bedaque and U. van Kolck, Ann. Rev. Nucl. Part. Sci. **52**, 339 (2002), and references therein.

[17] E. Epelbaum, Prog. Part. Nucl. Phys. **57**, 654 (2006), and references therein.

[18] R. Machleidt, K. Holinde and C. Elster, Phys. Rep. **149**, 1 (1987); R. Machleidt, Phys. Rev. C, **63**, 024001 (2001).

[19] V.G.J. Stoks, R.A.M. Klomp, C.P.F. Terheggen and J.J. de Swart, Phys. Rev. C, **21**, 861 (1980); Phys. Rev. C, **49**, 2950 (1994).

[20] Y Kim, I. Danchev, K. Kubodera, F. Myhrer and T. Sato, Phys. Rev. C, **73**, 025202 (2006).